Combined Parameter and State Estimation Problem in a Complex Domain: RF Hyperthermia Treatment Using Nanoparticles

L A Bermeo Varon[1], H R B Orlande[1] and G E Eliçabe[2],
[1] Federal University of Rio de Janeiro, Department of Mechanical Engineering, PEM/COPPE, Rio de Janeiro, RJ, Brazil
[2] University of Mar del Plata, Institute of Materials Science and Technology, INTEMA, Mar del Plata, Argentina

E-mail: lebermeo@ufrj.br; helcio@mecanica.coppe.ufrj.br; elicabe@fi.mdp.edu.ar

Abstract. The particle filter methods have been widely used to solve inverse problems with sequential Bayesian inference in dynamic models, simultaneously estimating sequential state variables and fixed model parameters. This methods are an approximation of sequences of probability distributions of interest, that using a large set of random samples, with presence uncertainties in the model, measurements and parameters. In this paper the main focus is the solution combined parameters and state estimation in the radiofrequency hyperthermia with nanoparticles in a complex domain. This domain contains different tissues like muscle, pancreas, lungs, small intestine and a tumor which is loaded iron oxide nanoparticles. The results indicated that excellent agreements between estimated and exact value are obtained.

1. Introduction

The particle filter methods which became widely used to solve inverse problems of sequential Bayesian inference in dynamic models are of great interest for different practical applications. In these applications, the available measured data are used together with prior knowledge about the physical phenomena and the measuring devices, in order to sequentially produce estimates of the desired dynamic variables [1].

In the order side, the hyperthermia is a cancer treatment where the tumor tissue it is heated to high temperatures, frequently between 40°C and 47°C, and the heating imposed is carried out by induction of electromagnetic waves [2]. Currently, the hyperthermia treatment with nanoparticles loaded into the tumorous cells it is being studied, this treatment can concentrate the temperature increase in the tumor region, thus not resulting on damages to the healthy tissues [3–10].

Currently, the particle filter methods have been used in the analysis of radiofrequency hyperthermia treatment with nanoparticles providing excellent results in state estimation [4] and simultaneous parameter and state estimation [9,11] in simple geometries. In this paper the particle filter is extended to combined parameter and state estimation in a complex domain by the proposal of Liu & West [12].

[1] To whom any correspondence should be addressed.

2. Parameter and state estimation problem

In the parameter and state estimation problem, consider a model for the evolution given by [13]:

$$\mathbf{x}_k = \mathbf{f}_k\left(\mathbf{x}_{k-1}, \boldsymbol{\theta}, \mathbf{v}_{k-1}\right) \tag{1}$$

where the subscript $k = 1, 2, ...,$ denotes a time instant t_k in a dynamic problem. The vector $\mathbf{x} \in R^{n_x}$ is the state vector and contains the variables to be dynamically estimated and $\mathbf{f}_k$ is a general function of the state variables $\mathbf{x}$, of the vector of parameters $\boldsymbol{\theta}$ and of the state noise vector $\mathbf{v}_{k-1}$ [13].

The measurements $\mathbf{z}_k \in R^{n_z}$ are available at t_k, $k = 1, 2, ...,$ and are related to the state variables $\mathbf{x}_k$ through the observation model given by:

$$\mathbf{z}_k = \mathbf{h}_k\left(\mathbf{x}_k, \boldsymbol{\theta}, \mathbf{n}_k\right) \tag{2}$$

where $\mathbf{h}_k$ is a function of the state variables $\mathbf{x}$, of the parameters $\boldsymbol{\theta}$ and measurement noise $\mathbf{n} \in R^D$.

This paper considered the filtering form of the state estimation problem. By assuming that $\pi(\mathbf{x}_0 \mid \mathbf{z}_0, \boldsymbol{\theta}) = \pi(\mathbf{x}_0)$ is available at time t_0, $\pi(\mathbf{x}_k \mid \mathbf{z}_{1:k}, \boldsymbol{\theta})$ is obtained with Bayesian filters in two sequential steps, prediction and update. In the prediction step, the state evolution model is used to advance the vector of state variables from time t_{k-1} to time t_k, providing a prior distribution $\pi(\mathbf{x}_k)$ for the state variables at time t_k. In the update step, the information provided by the measurements is then adjoined to this prior distribution through Bayes' theorem, by using the likelihood function $\pi(\mathbf{z}_k \mid \mathbf{x}_k, \boldsymbol{\theta})$ [1].

The Particle Filter method is a Monte Carlo technique, where the required posterior density function is represented by a set of random samples with associated weights; the statistics of the posterior distribution is computed based on these samples and weights [1]. Let $\mathbf{x}_k^i$ denote the particle *i*, with associated weight $w_k^i, i = 0,..., N$ at time t_k. Also let the set of all state variables $\mathbf{x}_{0:k} = \{\mathbf{x}_j, j = 0,1,...,k\}$ up to t_k, where *N* is the number of particles. The weights are normalized so that $\sum_{i=1}^{N} w_k^i = 1$. Then, the posterior marginal distribution, can be approximated by [1]:

$$\pi(\mathbf{x}_k \mid \mathbf{z}_k, \boldsymbol{\theta}) \approx \sum_{i=1}^{N} w_k^i \delta(\mathbf{x}_k - \mathbf{x}_k^i) \tag{3}$$

with weights computed from:

$$w_k^i \propto w_{k-1}^i \pi(\mathbf{z}_k \mid \mathbf{x}_k^i, \boldsymbol{\theta}) \tag{4}$$

The algorithm by Liu & West [12], which is based on the auxiliary sample importance resampling (ASIR) version of the particle filter [14], can be used for the estimation of the posterior probability distribution $\pi\left(\mathbf{x}_k, \boldsymbol{\theta} \mid \mathbf{z}_{1:k}\right)$. The particles are represented to $\{\mathbf{x}_k^i, \boldsymbol{\theta}_k^i : i = 0,..., N\}$ and the particle filter is based on the hypothesis that the vector of non-dynamic parameters $\boldsymbol{\theta}$ is represented by [15]:

$$\pi(\boldsymbol{\theta} \mid \mathbf{z}_{1:k-1}) \approx \sum_{i=1}^{N} w_{k-1}^i \, \mathrm{N}(\boldsymbol{\theta} \mid \mathbf{m}_{k-1}^i, h^2 \mathbf{V}_{k-1}) \tag{5}$$

where $\mathrm{N}(\boldsymbol{\theta}; \mathbf{a}, \mathbf{B})$ is a multivariate normal density with mean a and covariance matrix B, while *h* is a smoothing factor and $\mathbf{V}_{k-1}$ is the Monte Carlo posterior covariance matrix at time t_k. Equation (5)

shows that the above density is a mixture of Gaussian $\mathrm{N}(\boldsymbol{\theta}|\mathbf{m}_{k-1}^{i}, h^2\mathbf{V}_{k-1})$ distributions weighted by the sample weights w_{k-1}^{i}. The Gaussian kernel centers $\mathbf{m}_{k-1}$ are specified by the shrinkage rule [15]:

$$\mathbf{m}_{k-1}^{i} = a\,\boldsymbol{\theta}_{k-1}^{i} + (1-a)\bar{\boldsymbol{\theta}}_{k-1} \tag{6}$$

where $\bar{\boldsymbol{\theta}}_k$ is the mean of $\boldsymbol{\theta}$ at time t_k. The shrinkage factor is computed by:

$$a = \frac{3\delta - 1}{2\delta} \tag{7}$$

where $0.95 < \delta < 0.99$ is a discount factor. The smoothing factor h, also depends on the shrinkage factor, as follows:

$$h^2 = 1 - a^2 \tag{8}$$

Table 1. Liu and West's algorithm [12].

Select a value for $\delta \in [0.95; 0.99]$, then compute a with equation (7) and h^2 with equation (8);
For i =1, …, N Compute $\mathbf{m}_{k-1}^{i}$ with Equation (6) and calculate $\mu_k^i = E[\mathbf{x}_k \mid \mathbf{x}_{k-1}^{i}, \mathbf{m}_{k-1}^{i}]$.
Calculate the weights with likelihood density $\mathbf{w}_k^i = \pi(\mathbf{z}_k \mid \mu_k^i, \mathbf{m}_{k-1}^{i})\mathbf{w}_{k-1}^{i}$.
Calculate the total weight $t = \sum_i \mathbf{w}_k^i$; Normalize the particle weights, for i = 1, ..., N let $\mathbf{w}_k^i = t^{-1}\mathbf{w}_k^i$.
Construct the cumulative sum of weights (CSW) by $c_i = c_{i-1} + \mathbf{w}_k^i$ for i = 1,...,N with $c_0 = 0$
Let i = 1 and draw a starting point u_1 from the uniform distribution U[0,N^{-1}]
For j = 1, ... , N Move along the CSW by making $u_j = u_1 + N^{-1}(j-1)$
While $u_j > u_i$ make $i = i + 1$; Assign parent $i^j = i$.
For j = 1, ..., N Draw samples $\boldsymbol{\theta}_k^j$ from $\mathrm{N}(\boldsymbol{\theta}_k^j \mid \mathbf{m}_{k-1}^{ij}, h^2\mathbf{V}_{k-1})$, by using the parent ij.
For j = 1, ..., N Draw particles $\mathbf{x}_k^j$ from the prior density $\pi(\mathbf{x}_k \mid \mathbf{x}_{k-1}^{ij}, \boldsymbol{\theta}_k^j)$, by using the parent ij,
Calculate the correspondent weights $w_k^j = \frac{\pi(\mathbf{z}_k \mid \mathbf{x}_k^j, \boldsymbol{\theta}_k^j)}{\pi(\mathbf{z}_k \mid \mu_k^{ij}, \mathbf{m}_k^{ij})}$, with likelihood density
Calculate the total weight $t = \sum_i \mathbf{w}_k^i$; Normalize the particle weights, for i = 1, ..., N let $\mathbf{w}_k^i = t^{-1}\mathbf{w}_k^i$.

3. Physical Problem and mathematical formulation

The physical problem considered involves a 2D complex domain that consists of different biological healthy tissues like muscle, pancreas, lungs, small intestine, fat, arteries, vertebrae and a tumor loaded of iron oxide nanoparticles. Thermophysical properties in the tissues are constant and two external electrodes for induction of radiofrequency are considered, the physical problem is shown in Figure 1. The electric potential within the domain can obtained by solving the Laplace's equation [16]:

$$\nabla \cdot \left[\varepsilon(\mathrm{X}) \cdot \nabla\varphi(\mathrm{X})\right] = 0 \tag{10}$$

where φ is the potential; ε is the permittivity and X are the Cartesian coordinates, this is X = (x,y). The interfaces between the tissues are assumed to have ideal electric contact. The boundary conditions on the surface of the domain are given by:

$$\varphi(\mathrm{X}) = U \quad \text{at } \Omega_1' \tag{11}$$

$$\varphi(\mathrm{X}) = 0 \quad \text{at } \Omega_2' \tag{12}$$

$$\nabla\varphi(\mathrm{X}) \cdot \mathbf{n} = 0 \text{ elsewhere over the boundary} \tag{13}$$

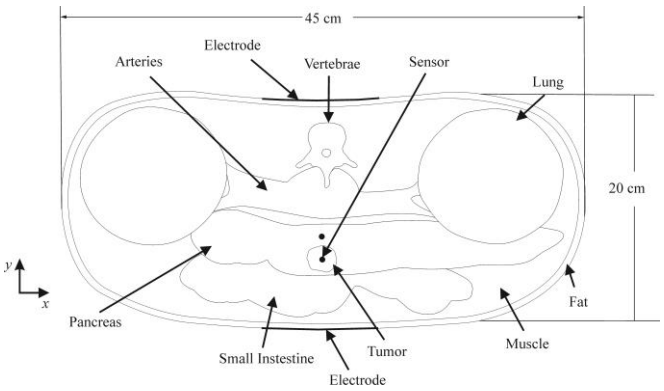

Figure 1. System Domain

where U denote the electric potential, Ω_1' is the upper electrode and Ω_2' is the lower electrode. The electric field strength **E** and the magnetic field **H** are obtained by:

$$\mathbf{E}(\mathrm{X}) = -\nabla\varphi(\mathrm{X}) \tag{14}$$

$$\left|\mathbf{H}(\mathrm{X})\right| = \frac{1}{1+N(\chi)}\frac{\left|\mathbf{E}(\mathrm{X})\right|}{\mu_0 \pi f R} \tag{15}$$

where $N(\chi) = 1/3$ is the demagnetizing factor of the composite tissue [17], χ is the susceptibility of the magnetic nanoparticles that can be described in terms of complex susceptibility $\chi = \chi' + i\chi''$ [18], μ_o is the dielectric constant permeability of free space (μ_o=4π x $10^{-7}\mathrm{T}\cdot\mathrm{m}\cdot\mathrm{A}^{-1}$), f is the electromagnetic frequency and R is the radius of magnetic induction loop. The electric heat source in the tissues that do not contain nanoparticles is given by [16]:

$$Q_{e_x}(\mathrm{X}) = \frac{\sigma_x \left|\mathbf{E}(\mathrm{X})\right|^2}{2} \tag{16}$$

where σ_x is the electric conductivity of the biological healthy tissue. The contribution for the heat source resulting from the presence of the magnetic nanoparticles is [18]:

$$Q_n = \mu_0 \pi f \chi'' \left|\mathbf{H}(\mathrm{X})\right| \tag{17}$$

Thus, the heat source in the tumor due to induction of magnetic nanoparticles is calculated by [17]:

$$Q_{e_y}(\mathrm{X}) = (1-\theta)\frac{\sigma_y \left|\mathbf{E}(\mathrm{X})\right|^2}{2} + \theta\left[\frac{9}{16}\frac{\chi''}{\mu_0 \pi f R^2}\left|\mathbf{E}(\mathrm{X})\right|^2\right] \tag{18}$$

where $\theta = n\pi r^2 / A$ is the concentration of nanoparticles, r is the mean radius of the supposedly spherical nanoparticles, n is the number of nanoparticles, A is the area of the tumor and σ_y is the electrical conductivity of the tumor embedded with nanoparticles, which can be approximated by a serial arrangement of the two materials, this is, $1/\sigma_y = (1-\theta)/\sigma'_y + \theta/\sigma_n$, where σ'_y and σ_n are the electrical conductivity of tumor and nanoparticles, respectively. The permittivity of the tumor tissue embedded with nanoparticles is approximated by $\varepsilon_y = \varepsilon'_y$, where ε'_y is permittivity of the tumor, since the concentration of particles is too small and differences in this parameter for biological tissue and nanoparticles are not evidently large.

The mathematical formulation for bioheat transfer in this study is described by Pennes's Equation [19]:

$$\rho(\mathrm{X})c_p(\mathrm{X})\frac{\partial T(\mathrm{X},t)}{\partial t}=\nabla\cdot\left[k(\mathrm{X})\nabla T(\mathrm{X},t)\right]+\rho_b c_{p,b}\omega_b(\mathrm{X})\left[T_b-T(\mathrm{X},t)\right]+Q_m(\mathrm{X})+Q_e(\mathrm{X}) \quad (19)$$

where ρ is the density, c_p is the specific heat, k is the thermal conductivity, ρ_b is the blood density, $c_{p,b}$ is the specific heat of blood, ω_b is the blood perfusion rate, T_b is the blood temperature, Q_m is the metabolic heat source and Q_e is the electrical heat source generated by radiofrequency external excitation given by equations (16) and (18). The interfaces between biological healthy tissues are assumed to be in ideal thermal contact and the thermal boundary conditions are given by:

$$\begin{cases} -k(\mathrm{X})\dfrac{\partial T(\mathrm{X})}{\partial x}=0 & \text{at } x=0, x=L_x, 0<y<L_y, t>0 \\ -k(\mathrm{X})\dfrac{\partial T(\mathrm{X})}{\partial y}=h_f\left(T(\mathrm{X})-T_f\right) & \text{at } y=0, y=L_x, 0<x<L_x, t>0 \end{cases} \quad (20)$$

where h_f is the heat transfer coefficient, T_f is the temperature of the surrounding medium, L_x and L_y are the domain lengths in the x and y directions. The initial temperature T_0 is considered constant.

4. Results and discussions

A 2D complex domain considered is shown in Figure 1. The lengths of both electrodes are 20 cm. Thermophysical properties of the biological healthy tissues and tumor, and the electrical properties considering a frequency f = 1 MHz are described in Table 2. For the convective boundary condition we assume T_f = 20°C, and h_f = 45 W/(m^2.K). The initial condition is taken as the uniform temperature T_0 = 37°C. For the iron oxide nanoparticles (Fe_3O_4) that are assumed to be uniformly distributed into the tumor, the following parameters have been considered: k_n = 40 W/(m.K), $c_{p,n}$ = 4000 J/(kg.K), ρ_n = 5180 kg/m^3 , σ_n = 25000 S/m, ε_n = ε_y and magnetic susceptibility χ'' = 18 , with n = 8x10^{10} nanoparticles of radius r = 10^{-8} m. The thermal properties for the tumor embedded with nanoparticles was approximated by the rule of mixture [17].

Table 2. Thermophysical and Electrical Properties [20].

Parameter	Pancreas	Small Intestine	Lung	Muscle	Fat	Vertebrae	Arteries	Tumor
Thermal Conductivity (k) W/(m.K)	0.51	0.49	0.39	0.49	0.21	0.32	0.46	0.75[2]
Specific Heat (c_p) J/(kgK)	3164	3595	3886	3421	2348	1313	3306	3164[1]
Density (ρ) kg/m^3	1087	1030	394	1090	911	1908	1102	1087[1]
Perfusion Coefficient (ω) s^{-1}	0.01389	0.01761	0.00263	0.0006	0.0005	0.0003	0.0027	0.02
Metabolic Heat Source (Q_m) W/m^3	12924.43	16366.7	2446.74	991.9	464.61	286.2	2556.64	42000[2]
Electrical Conductivity (σ) S/m	0.603	0.865	0.136	0.503	0.0441	0.00244	0.327	0.723[2]
Permittivity (ε)	1430	5680	733	1840	50.8	145	218	1716[2]

[1] thermal properties of pancreas. [2] [4]

The direct problem solution is analyzed without and with nanoparticles of Fe_3O_4, the applied voltage on the upper electrode is 10V with respect to ground, the lower electrode maintained to ground, during 900s. Figure 2.a presents the transient temperature inside the tumor, at the position x = 22.5 cm and y = 5 cm. For the case without nanoparticles, the maximum temperature is 38.78°C, and the temperature increase does not reach levels of hyperthermia. For the case with nanoparticles inside tumor, the maximum temperature is 44.34°C, which, reveals that the use of nanoparticles in the tumor increase the temperature substantially in this region while keeping the other regions at lower temperatures (see Figure 2.b for the temperature in the pancreas at the position x = 22.5 cm and y = 7 cm).

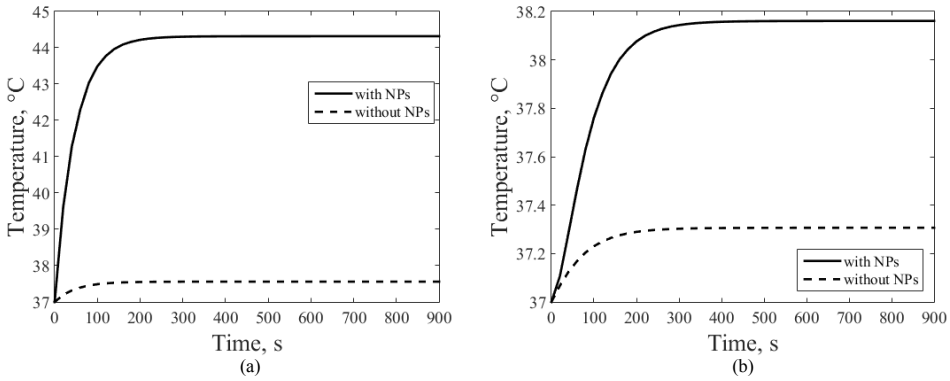

Figure 2. Transient Temperature (a) in Tumor (sensor position), (b) in Pancreas.

For the solution of the parameter and state estimation problem, one single sensor was assumed available for the inverse analysis, located inside the tumor. The measurements were generated from the solution of the direct problem with the parameters specified above. Uncorrelated Gaussian errors with zero mean and standard deviation of 1°C were then added to the solution. The simulated measurements were supposed available every 20s.

The evolution model for the electric field was taken in the form of a random walk, that is, for each particle *i,* was added a Gaussian random variable with zero mean and a standard deviation of 10% of the deterministic solution of the electrical problem

Gaussian uncorrelated noise with zero mean and a standard deviation of 1°C was also added to the solution of the bioheat transfer problem, which served as the evolution model for the temperature.

The prior probability densities for the parameters $\boldsymbol{\theta}$ were assumed as Gaussians, with zero mean and standard deviation of 10% of the mean value of each parameter. The vector of parameters is given by

$$\boldsymbol{\theta} = [k_x, k_y, c_{p,b}, c_{p,x}, c_{p,y}, \rho_b, \rho_x, \rho_y, \omega_{b,x}, \omega_{b,y}, Q_{m,x}, Q_{m,y}, h_f, \sigma_x, \sigma_y, n, r, \chi''] \tag{21}$$

where the subscript *x* indicated the properties of biological healthy tissue (pancreas, small intestine, lung, muscle, fat, vertebrae and arteries) which are different for each of these, the subscript *y* indicate the properties of tumor embedded with nanoparticles.

The effects of the number of particles on the estimation of parameter and state variables were examined by using 50, 100 and 250 particles. The accuracy of the estimation of state variables was addressed in terms of the means and standard deviations of the root mean square error (RMS), obtained with thirty repetitions of Liu & West's algorithm. Table 3 shows the means and standard deviation values of the thirty repetitions of the particle filter, for each case examined. It is observed that the means and standard deviations of the RMS error decrease when the number of particles is increased, as expected.

Table 3. RMS results.

Number of Particles	$\overline{\text{RMS}}$	Standard Deviation
50	0.835	0.423
100	0.727	0.395
250	0.601	0.378

Figure 3.a shows the transient temperature at the tumor (sensor position) obtained with the Liu & West's algorithm of particle filter with 100 particles, where we note that the estimated temperature is

in better agreement with the exact solution than the measurements. Figure 3.b presents the transient temperature inside the pancreas (no available measures). It is observed that the estimated temperature is in excellent agreement with the exact temperature. In this case, although is observed a great RMS errors; note in these figures that the temperatures can be quite accurately estimated.

Figure 4 shows the evolution in time of selected parameters with 100 particles. Note that the estimated means are in excellent agreement with the exact ones, even with only 100 particles. Although the great uncertainties in the measurements and in the evolution and observation models. Observe, the uncertainties related to the parameters have a propensity to decrease as time evolves and more information becomes available for the solution. Indeed, the results presented above show that both parameters and state variables could be accurately recovered with Liu & West's algorithm of the particle filter.

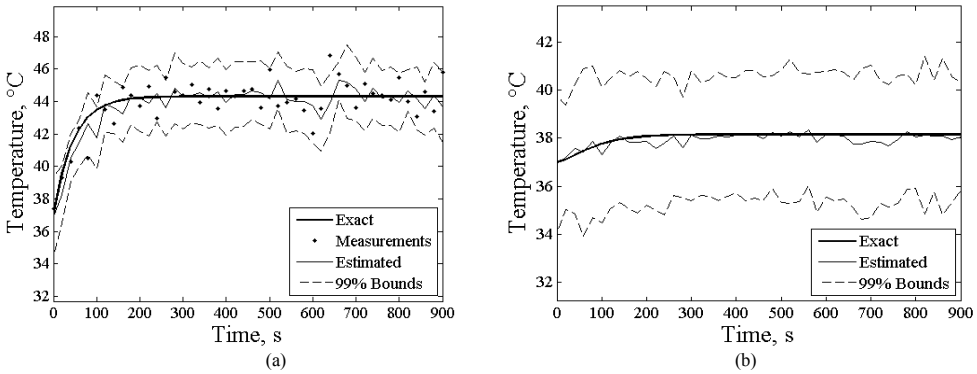

Figure 3. Estimated Transient Temperature (a) in Tumor (sensor position), (b) in Pancreas.

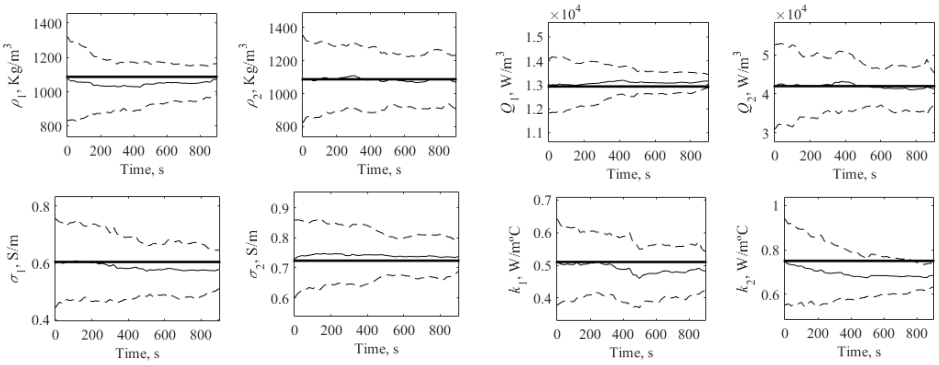

Figure 3. Estimated parameters values: exact (dark black lines), estimated (black lines) and 99% bonds (dashed lines), subscript 1 are the pancreas properties and 2 are the tumor properties.

5. Conclusions

The accuracy of the particle filter algorithm for combined parameter and state estimation was applied to the estimation of the temperature field in radiofrequency hyperthermia with magnetic nanoparticles of iron oxide, using one single measurement, in a 2D complex geometry. Excellent results were obtained for the estimations of parameters and state variables, with large uncertainties and small number of particles, even in locations where no measurements are available. The results presented herein are expected to contribute for future temperature control in the hyperthermia treatment.

Acknowledgments

The financial support provided by FAPERJ, CAPES and CNPq.

References

[1] Kaipio J P and Somersalo E 2004 *Computational and Statistical Methods for Inverse Problems* (Berlin, Heidelberg: Springer)
[2] Miaskowski A and Sawicki B 2013 Magnetic fluid hyperthermia modeling based on phantom measurements and realistic breast model. *IEEE Trans. Biomed. Eng.* **60** 1806–13
[3] Kurgan E and Gas P 2015 Simulation of the electromagnetic field and temperature distribution in human tissue in RF hyperthermia *Prz. Elektrotechniczny* **1** 171–4
[4] Bermeo Varon L A, Orlande H R B and Elicabe G 2015 Estimation of state variables in the hyperthermia therapy of cancer with heating imposed by radiofrequency electromagnetic waves *Int. J. Therm. Sci.* **98** 228–36
[5] Dombrovsky L A, Timchenko V, Jackson M and Yeoh G H 2011 A Combined Transient Thermal Model for Laser Hyperthermia of Tumors with Embedded Gold Nanoshells *Int. J. Heat Mass Transf.* **54** 5459–69
[6] Lamien B, Orlande H R B, Elicabe G E and Maurente A J 2014 State Estimation Problem in Hyperthermia Treatment of Tumors Loaded with Nanoparticles *Proceedings of the 15th International Heat Transfer Conference, IHTC-15* (Kyoto, Japan) pp 1–15
[7] Kurgan E and Gas P 2011 Treatment of Tumors Located in the Human Thigh using RF Hyperthermia *Prz. Elektrotechniczny* **87** 103–6
[8] Gas P and Miaskowski A 2015 Specifying the ferrofluid parameters important from the viewpoint of Magnetic Fluid Hyperthermia *Sel. Probl. Electr. Eng. Electron. IEEE Xplore Digit. Libr.* 1–6
[9] Bermeo Varon L A, Orlande H R B and Eliçabe G E 2015 Combined Parameter and State Estimation in the Radiofrequency Hyperthermia Treatment of Cancer *Heat Transf. Part A Apl.* **accept** 1–31
[10] Lamien B, Bermeo Varon L A, Orlande H R B and Eliçabe G E 2016 State Estimation in Bioheat Transfer: a Comparison of Particle Filter Algorithms *Int. J. Numer. Methods Heat Fluid Flow* **Submitted** 1–40
[11] Lamien B, Orlande H R B and Eliçabe G E 2015 Comparison of Particle Filter Algorithms Applied to the Temperature Filed Estimation in Hyperthermia Phantoms *1st Thermal and Fluid Engineering Summer Conference, ASTFE, 2015* (New York, New York, USA) p TFESC – 13764
[12] Liu J and West M 2001 Combined parameter and state estimation in simulation based filtering *Sequential Monte Carlo Methods in Practice* ed S A. Doucet, N. de Freitas, and N. Gordon, (Eds.), New York pp 197–217
[13] Arulampalam M S, Maskell S, Gordon N and Clapp T 2002 A tutorial on particle filters for online nonlinear/non-Gaussian Bayesian tracking *IEEE Trans. Signal Process.* **50** 174–88
[14] Pitt M K and Shephard N 1999 Filtering via Simulation: Auxiliary Particle Filters *J. Am. Stat. Assoc.* **94** 1–41
[15] West M 1993 Approximating Posterior Distributions by Mixture *J. R. Stat. Soc. B* 409–22
[16] Cheng D K 1993 *Fundamentals of Engineering Electromagnetics* (United State of America: Addison-Wesley Publishing Company, Inc)
[17] Andra W, Ambly C G, Hergt R, Hilger I and Kaiser W A 1999 Temperature distribution as function of time around a small spherical heat source of local magnetic hyperthermia *J. Magn. Magn. Mater.* **194** 197–203
[18] Rosensweig R E 2002 Heating magnetic fluid with alternating magnetic field *J. Magn. Magn. Mater.* **252** 370–4
[19] Pennes H H 1948 Analysis of tissue and arterial blood temperatures in the resting human forearm. 1948. *J. Appl. Physiol.* **1** 93–124
[20] Hasgall P ., Di Gennaro F, Baumgartner C, Neufeld E, Gosselin M ., Payne D, Klingenböck A and Kuster N 2015 IT'IS Database for thermal and electromagnetic parameters of biological tissues *Version 3.0*